MAGNETIC FLUX DETECTING OF BEARINGLESS INDUCTION MOTORS WITH SEARCH COILS

Xiao-lin Wang, Zhi-quan Deng, Ying-jie Lin, Yang-guang Yan
University of Aeronautics and Astronautics,
College of Automation Engineering, Nanjing, China, 210016
wangxl@nuaa.edu.cn

ABSTRACT

The magnetic force of bearingless induction motors is generated with two kinds of magnetic fields interaction. The levitated mechanism determines the strong coupling relation between the air-gap flux of drive winding and that of levitation winding. Then it is very important to estimate or detect the distribution of magnetic flux. In this paper, as different positions of search coils are concerned, three methods of detecting the air gap flux density are analyzed in detail: evenly distributed angle position method, typical angle position method and analytic method. Moreover, the principle of the levitated force production is introduced. The control system configuration is proposed. At last, parameters of the motor prototype are given. The experimental results verify the validity of the proposed methods.

INTRODUCTION

The interest in ultra-speed motors and generators in industry applications is increasing recently. Bearingless motors, which combine magnetic levitation bearings with the drive winding, have the advantage of no abrasion, no lubrication and no particle generation caused by bearings. Furthermore, in comparison with conventional magnetic bearing motors, the axial length of the rotor is decreased, which results in increased frequency of the mechanical natural vibration, and the efficiency can be increased because the magnetic flux of the motor can partly be used for levitation.

In recent years, a universal controller for bearingless induction motors has been proposed based on field oriented vector, such as air-gap flux orientation and rotor flux orientation[1]~[6]. However, there remain some limitations in the control algorithm:

1) Normal speed sensors are very expensive and none meets the measurement precision under the ultra-speed running. For example, the maximum speed of photoelectric encoder is lower than 10,000 r/min.

2) There is great difficulty in realizing the adaptive control or sensorless control, and restriction of the inherent maximal pullout torque because of complexity of the control computation. [7][8]

3) The control system requires an information link between the drive controller and the levitation one. Therefore, the low cost general-purpose inverter sold in the market cannot be used in this situation.

For these reasons, the independent control of levitated subsystem has to be built. In addition, in order to control the radial force, it is very important to detect or estimate the distribution of the magnetic flux densities in the air-gap of bearingless induction motors.

In early 2000, the method of detecting the amplitude and orientation of the air-gap magnetic field has been proposed with search coils wound around stator teeth of bearingless induction motors.[9][10] However, these flux components calculation based on search coil has not reported in detail.

In this paper, three calculation methods of detecting the air-gap flux are analyzed in detail: evenly distributed angle position method, typical angle position method and analytic method. In other words, the air-gap flux densities B_1 of the drive winding and B_2 of the levitation winding can be detected respectively with search coils. To the author's best knowledge, the analytic method has not yet been published in literature before.

PRINCIPLE AND CONTROL SYSTEM

According to [1], by combining 3-phase drive winding with pole pair number p_1 and 3-phase levitation winding with pole pair number $p_2 = p_1 \pm 1$ and keeping their angular velocity of revolving magnetic field: $\omega_1 = \omega_2$, Maxwell force is generated for radial force in the induction motor.

Fig.1 shows MMFs of two sets of windings of the bearingless induction motor. If $p_2 = p_1 + 1$, the rotor angular velocity ω_r controlled by drive winding is

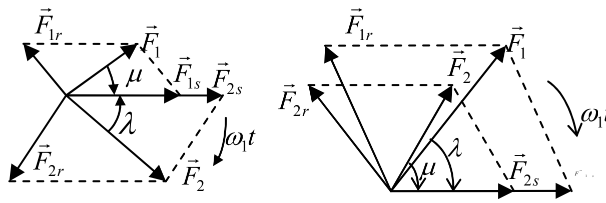

(a) $p_2 = p_1 + 1$ (b) $p_2 = p_1 - 1$

Fig.1 MMFs of drive winding and levitation winding

larger than the synchronous angular velocity ω_2, then the levitation winding operates as a generator. The stator's MMF $\vec{F}_{2s}$ lags behind the air-gap's MMF $\vec{F}_2$. On the contrary, if $p_2 = p_1 - 1$, the levitation winding operates as a motor. Then there is a phase delay of the rotor's MMF $\vec{F}_{2r}$ to the air-gap's MMF $\vec{F}_2$. When the axes of A-phase of two windings overlap each other, their stators' MMFs are unanimous in the direction.

According to the general theory of motor control, if the drive winding is executed by sinusoidal current, its stator MMF $f_{1s}(\varphi, t)$ can be written as

$$f_{1s}(\varphi,t) = F_{1s}\cos(\omega_1 t - p_1\varphi) \tag{1}$$

where F_{1s} is the peak value of the stator MMF, φ is the space position angle.

The air-gap flux density produced by the drive winding is given by

$$B_1(\varphi,t) = B_{1m}\cos(\omega_1 t - p_1\varphi - \mu) \tag{2}$$

where B_{1m} is the peak value of the air-gap flux density, μ is the phase angle from $\vec{F}_1$ to $\vec{F}_{1s}$.

Similarly, the air-gap flux density of the levitation winding can be written as

$$B_2(\varphi,t) = B_{2m}\cos(\omega_2 t - p_2\varphi - \lambda) \tag{3}$$

where B_{2m} is the peak value of the air-gap flux density; λ is the phase angle from $\vec{F}_2$ to $\vec{F}_{2s}$.

Then the total flux density in the air-gap is shown as (4), the summation of (2) and (3)

$$\begin{aligned} B(\varphi,t) = {} & B_{1m}\cos(\omega_1 t - p_1\varphi - \mu) \\ & + B_{2m}\cos(\omega_2 t - p_2\varphi - \lambda) \end{aligned} \tag{4}$$

Substituting equation (4) into the Maxwell Forces in α- and β- direction as follows

$$\left.\begin{aligned} F_\alpha &= \int_0^{2\pi} \frac{lR}{2\mu_0} B^2(\varphi,t)\cos\varphi d\varphi \\ F_\beta &= \int_0^{2\pi} \frac{lR}{2\mu_0} B^2(\varphi,t)\sin\varphi d\varphi \end{aligned}\right\} \tag{5}$$

where l is the active length of the rotor, R is the rotor radius, and μ_0 is the vacuum or air permeability.

For the rotor current of the levitation winding is neglected, the air-gap flux density is expressed as

$$B_2 \approx \frac{p_2 L_{2m}}{2lRW_2} i_2 \tag{6}$$

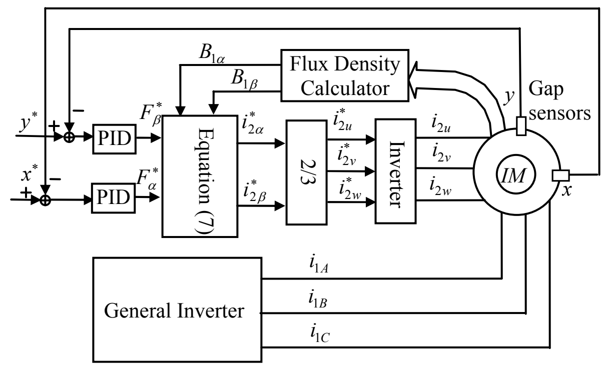

Fig.2 An independent control system of the levitation winding of bearingless induction motors

where L_{2m} is the mutual inductance of the levitation winding. W_2 is the number of turns for the levitation winding.

In this paper, $p_1 = 1, p_2 = 2$, then equation(5) can be simplified by equation (6) as

$$\begin{bmatrix} F_\alpha \\ F_\beta \end{bmatrix} = \sqrt{\frac{1}{24}} \frac{\pi L_{2m}}{W_2 \mu_0} \begin{bmatrix} B_{1\alpha} & B_{1\beta} \\ -B_{1\beta} & B_{1\alpha} \end{bmatrix} \begin{bmatrix} i_{2\alpha} \\ i_{2\beta} \end{bmatrix} \tag{7}$$

Fig.2 shows a block diagram of the proposed bearingless induction motor, the air-gap flux density components $B_{1\alpha}$ and $B_{1\beta}$ of the drive winding are calculated by detection block. In this situation, the control system of the levitation winding can be controlled independently, while the drive winding can be driven by general-purpose inverter.

FLUX DETECTION

In the bearingless induction motor, two sets of 3-phase windings are wound in the same stator slots: conventional $2p_1$ poles drive winding and additional $2p_2 = 2(p_1 \pm 1)$ poles levitation winding. To detect the flux densities in the air-gap, search coils are wound around stator teeth at $\theta = 2\pi(j-1)/K$, $j = 1,2,\cdots,K$. If p_1 is even, then $K = 4p_1$; otherwise $K = 4p_2$. The flux densities are detected by integrating induced voltage of search coils

For example, the two-pole ($p_1 = 1$) driver winding and the four-pole ($p_2 = 2$) levitation winding are wound in the stator of a typical 24-slot induction motor in Fig.3, then search coils ($K = 4p_2 = 8$) are wound around stator teeth at θ=0º, 45º, 90º, 135º, 180º, 225º, 270º and 315º.

The analysis below is based on the assumptions that the flux distribution in the air-gap confronted the stator tooth is uniform and the fringing flux is negligible.

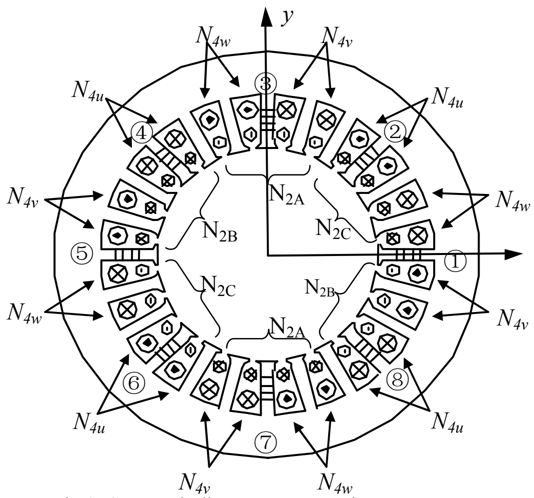

Fig.3 Stator winding arrangement in a motor prototype

When tooth flux density B_j is detected by using search coil, search coil terminal voltage V_{scj} is given as

$$V_{scj} = N_t S_t \frac{d}{dt} B_j \tag{8}$$

where N_t is the number of turns for a search coil; S_t is the tooth cross section area; $j = 1,2,\cdots,K$.

As a practical solution, a low-pass filter having a cut-off frequency f_c and a DC gain A are used as an incomplete integrator. Moreover, a high-pass filter having a time constant T is needed for eliminating the integrator drift due to measurement-offset error. A transfer function between the terminal voltage V_{scj} and the actual magnetic flux density B_j is given as

$$\frac{B_j}{V_{scj}} = \frac{1}{N_t S_t} \frac{2\pi f_c A}{s + 2\pi f_c} \frac{s}{s + \frac{1}{T}} \tag{9}$$

where $s = d/dt$.

The magnetic flux distribution vectors $B_{1\alpha}, B_{1\beta}$ of the drive winding and $B_{2\alpha}, B_{2\beta}$ of the levitation winding are calculated from the detected magnetic flux densities B_j . B_j can be calculated from the corresponding voltage V_{scj} according to equation(9).

A. Evenly Distributed Angle Position Method

In the negative ordinate Y-axis, the stationary angular position θ_m may be expressed as the corresponding θ_n in the positive Y-axis: $\theta_m = \theta_n + \pi$, where $m = n + K/2$, $n = 1,2,\cdots,K/2$. Then

$$\begin{aligned} &B_m \cos(p_1\theta_m) = B(\theta_n + \pi)\cos p_1(\theta_n + \pi) \\ &= B_{1\alpha}\cos^2(p_1\theta_n) + \tfrac{1}{2}B_{1\beta}\sin(2p_1\theta_n) \\ &- B_{2\alpha}\cos(p_2\theta_n)\cos(p_1\theta_n) \\ &- B_{2\beta}\sin(p_2\theta_n)\cos(p_1\theta_n) \end{aligned} \tag{10}$$

Substituting (10) into the summation as following

$$\begin{aligned} &\sum_{j=1}^{K} B_j \cos(p_1\theta_j) \\ &= \sum_{n=1}^{K/2} B_n \cos(p_1\theta_n) + \sum_{m=1+K/2}^{K} B_m \cos(p_1\theta_m) \end{aligned} \tag{11}$$

In this paper, $K = 4p_2$, p_2 is even number, then (11) can be simplified and the magnetic flux distribution vector $B_{1\alpha}$ of the drive winding is written as

$$B_{1\alpha} = \frac{2}{K}\sum_{j=1}^{K}[B_j \cos(p_1\theta_j)] \tag{12}$$

In the same way, the other distribution vectors $B_{1\beta}, B_{2\alpha}$ and $B_{2\beta}$ can be given as

$$B_{1\beta} = \frac{2}{K}\sum_{j=1}^{K}[B_j \sin(p_1\theta_j)] \tag{13}$$

$$B_{2\alpha} = \frac{2}{K}\sum_{j=1}^{K}[B_j \cos(p_2\theta_j)] \tag{14}$$

$$B_{2\beta} = \frac{2}{K}\sum_{j=1}^{K}[B_j \sin(p_2\theta_j)] \tag{15}$$

By the evenly distributed angle position method, $B_{1\alpha}, B_{1\beta}, B_{2\alpha}$ and $B_{2\beta}$ are obtained by calculating flux densities of all the search coils. Therefore, the harmonic effect can be suppressed in certain degree and the precision in calculation is improved**.** However, the algorithm is comparatively complicated and difficult to realize in digital control. Furthermore, the method is ineffective if there is something wrong with coils at any angle position.

B. Typical Angle Position Method

Apparently, the flux density in a stator tooth positioned at θ is obtained based on

$$\begin{aligned} B_j &= B_{1\alpha}\cos(p_1\theta_j) + B_{1\beta}\sin(p_1\theta_j) \\ &+ B_{2\alpha}\cos(p_2\theta_j) + B_{2\beta}\sin(p_2\theta_j) \end{aligned} \tag{16}$$

Then the air-gap flux densities toward the stator teeth at 0, $\frac{\pi}{2}$, π, $\frac{3\pi}{2}$, $B(\frac{\pi}{2p_2})$ and $B(\frac{\pi}{2p_2} + \pi)$ are written as

$$\left.\begin{aligned} &B(0) = B_{1\alpha} + B_{2\alpha} \\ &B(\pi) = -B_{1\alpha} + B_{2\alpha} \\ &B(\frac{\pi}{2}) = (-1)^{\frac{p_1-1}{2}} B_{1\beta} + (-1)^{\frac{p_2}{2}} B_{2\alpha} \\ &B(\frac{3\pi}{2}) = (-1)^{\frac{p_1+1}{2}} B_{1\beta} + (-1)^{\frac{p_2}{2}} B_{2\alpha} \\ &B(\frac{\pi}{2p_2}) = B_{1\alpha}\cos(\frac{p_1\pi}{2p_2}) + B_{1\beta}\sin(\frac{p_1\pi}{2p_2}) + B_{2\beta} \\ &B(\frac{\pi}{2p_2} + \pi) = B_{2\beta} - B_{1\alpha}\cos(\frac{p_1\pi}{2p_2}) - B_{1\beta}\sin(\frac{p_1\pi}{2p_2}) \end{aligned}\right\} \tag{17}$$

Sub-equations of (17) are added or subtracted, the magnetic flux distribution vectors B_1 of drive winding and B_2 of levitation winding in the perpendicular α- and β-axes are given as

$$\left.\begin{aligned} B_{1\alpha} &= \frac{B(0) - B(\pi)}{2} \\ B_{1\beta} &= (-1)^{\frac{p_1 - 1}{2}} \frac{B(\frac{\pi}{2}) - B(\frac{3\pi}{2})}{2} \\ B_{2\alpha} &= \frac{B(0) + B(\pi)}{2} \\ B_{2\beta} &= \frac{B(\frac{\pi}{2p_2}) + B(\frac{\pi}{2p_2} + \pi)}{2} \end{aligned}\right\} \tag{18}$$

Typical angle position method makes it possible to obtain the air-gap flux density components of two windings from the search coils at some certain angle positions. Each expression is simply determined by flux densities of search coils at two certain angular positions. Despite its advantage of easy realization, the results may be easily influenced by single search coil.

C. Analytic Method

In Fig.3, all of the air-gap flux densities confronted the search coils are obtained from (16) as

$$\begin{bmatrix} B_1 \\ B_2 \\ B_3 \\ B_4 \\ B_5 \\ B_6 \\ B_7 \\ B_8 \end{bmatrix} = \begin{bmatrix} 1 & 0 & 1 & 0 \\ \frac{\sqrt{2}}{2} & \frac{\sqrt{2}}{2} & 0 & 1 \\ 0 & 1 & -1 & 0 \\ -\frac{\sqrt{2}}{2} & \frac{\sqrt{2}}{2} & 0 & -1 \\ -1 & 0 & 1 & 0 \\ -\frac{\sqrt{2}}{2} & -\frac{\sqrt{2}}{2} & 0 & 1 \\ 0 & -1 & -1 & 0 \\ \frac{\sqrt{2}}{2} & -\frac{\sqrt{2}}{2} & 0 & -1 \end{bmatrix} \begin{bmatrix} B_{1\alpha} \\ B_{1\beta} \\ B_{2\alpha} \\ B_{2\beta} \end{bmatrix} \tag{19}$$

In the equations above, a linear equation with the variables of $B_1 \sim B_8$ established by eliminating the magnetic flux $B_{1\alpha}, B_{1\beta}, B_{2\alpha}$ and $B_{2\beta}$ is as follows

$$A\begin{bmatrix} B_1 & B_2 & B_3 & B_4 & B_5 & B_6 & B_7 & B_8 \end{bmatrix}' = 0 \tag{20}$$

where A is a 4×8 matrix,

$$A = \begin{bmatrix} -1 & \frac{\sqrt{2}}{2} & 0 & -\frac{\sqrt{2}}{2} & 1 & -\frac{\sqrt{2}}{2} & 0 & \frac{\sqrt{2}}{2} \\ 0 & \frac{\sqrt{2}}{2} & -1 & \frac{\sqrt{2}}{2} & 0 & -\frac{\sqrt{2}}{2} & 1 & -\frac{\sqrt{2}}{2} \\ 1 & 0 & 1 & 0 & 1 & 0 & 1 & 0 \\ 0 & 1 & 0 & 1 & 0 & 1 & 0 & 1 \end{bmatrix}$$

It is obvious that the rank of the matrix A is four, $r(A) = 4$. In other words, there are four ($K - r(A) = 4$) maximal linearly independent vectors (free vectors) in the fundamental solutions of equations, then the other vectors can be substituted by them. In addition, $B_{1\alpha}, B_{1\beta}, B_{2\alpha}$ and $B_{2\beta}$ can be calculated according to these free vectors. For example, the search coil flux densities B_2, B_4, B_6 and B_7 at θ of 45°, 135°, 225°, and 270° are maximal linearly independent vectors, then B_1, B_3, B_5 and B_8 can be written as

$$\begin{bmatrix} B_1 \\ B_3 \\ B_5 \\ B_8 \end{bmatrix} = \begin{bmatrix} -\frac{\sqrt{2}}{2} & -\sqrt{2} & -\frac{\sqrt{2}}{2} & -1 \\ \sqrt{2} & \sqrt{2} & 0 & 1 \\ -\frac{\sqrt{2}}{2} & 0 & \frac{\sqrt{2}}{2} & -1 \\ -1 & -1 & -1 & 0 \end{bmatrix} \begin{bmatrix} B_2 \\ B_4 \\ B_6 \\ B_7 \end{bmatrix} \tag{21}$$

Substituting equation (21) into (19), yields

$$\begin{bmatrix} B_{1\alpha} \\ B_{1\beta} \\ B_{2\alpha} \\ B_{2\beta} \end{bmatrix} = \begin{bmatrix} 0 & -\frac{\sqrt{2}}{2} & -\frac{\sqrt{2}}{2} & 0 \\ \frac{\sqrt{2}}{2} & \frac{\sqrt{2}}{2} & 0 & 0 \\ -\frac{\sqrt{2}}{2} & -\frac{\sqrt{2}}{2} & 0 & -1 \\ \frac{1}{2} & 0 & \frac{1}{2} & 0 \end{bmatrix} \begin{bmatrix} B_2 \\ B_4 \\ B_6 \\ B_7 \end{bmatrix} \tag{22}$$

It is proved that ten combinations (B_1, B_2, B_4, B_5), (B_1, B_2, B_6, B_7), (B_1, B_2, B_4, B_8), (B_1, B_3, B_5, B_7), (B_1, B_5, B_6, B_8), (B_2, B_3, B_5, B_6), (B_2, B_3, B_7, B_8), (B_2, B_4, B_6, B_8), (B_3, B_4, B_6, B_7), (B_4, B_5, B_7, B_8) are linearly dependent vectors, then there are totally $C_8^4 - 10 = 60$ available combinations on maximal linearly independent vectors.

Analytic method takes full advantage of relations between the air-gap flux density and all flux densities of search coils. By using this method, the air-gap flux density components $B_{1\alpha}, B_{1\beta}, B_{2\alpha}$ and $B_{2\beta}$ can be calculated from flux densities of search coils corresponding to the maximal linearly independent vectors, and the number of necessary search coils is minimized to the amount of the maximal linearly independent vectors.

In fact, both evenly distributed angle position method and typical angle position method are special forms of analytic method. They are the special solutions composed of certain maximal linearly independent vectors and other vectors in the analytic method.

EXPERIMENTAL RESULTS

In the paper, a bearingless induction motor prototype is designed. The parameters are as follows:

Active length of the rotor $l = 9.5\text{cm}$; rotor radius $R = 14.5\text{cm}$; weight of the rotor $m_r = 1\text{kg}$; clearance of the touch down bearing $\delta = 200\mu\text{m}$; number of turns for the drive winding $W_1 = 120$; number of turns for the levitation winding $W_2 = 32$; mutual inductance of the levitation winding $L_{2m} = 0.00435\text{H}$; cut-off frequency $f_c \approx 5\text{H}_\text{Z}$; DC gain $A = 0.414 \times 10^{-3}$; time constant $T = 0.064\text{s}$.

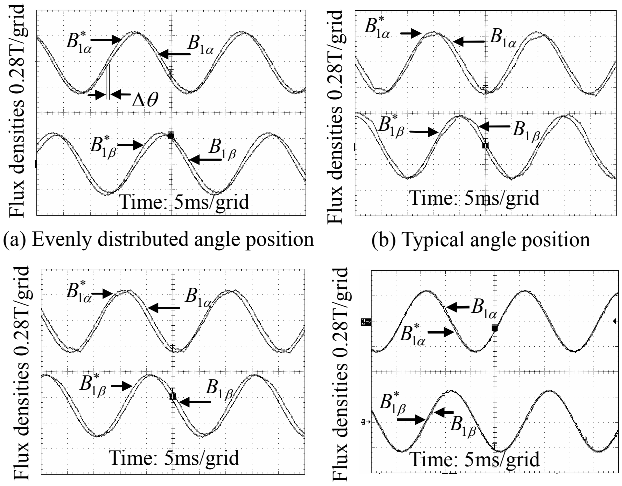

(a) Evenly distributed angle position (b) Typical angle position

(c) Analytic method (d) With the compensator

Fig.4 Waveforms of the air-gap flux densities of the drive winding

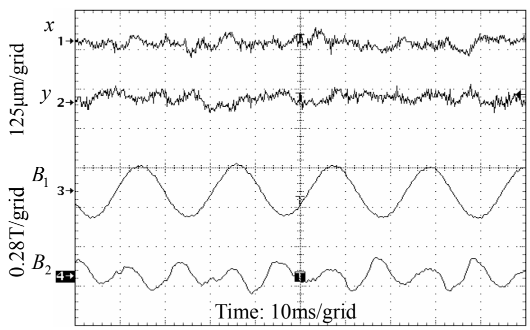

Fig.5 Waveforms of the independent levitated subsystem

To verify the validity of the methods proposed, the drive winding is controlled by the feasible air-gap flux orientation controller in [5][6]. Fig.4 (a)-(c) show the commands flux densities $B_{1\alpha}^*$ and $B_{1\beta}^*$ of the drive winding, as well as the air-gap flux density components $B_{1\alpha}$ and $B_{1\beta}$ calculated according to flux densities of search coils. There is a phase delay between calculated results and commands caused by the incomplete integrator, the filter and D/A sampling delay, etc. Then a phase lead-lag compensator is designed, and its effectiveness is shown in Fig.4 (d).

In addition, the drive winding is driven directly by normal 3-phase alternating-current supply. Therefore, the independent control of levitated subsystem with search coils has been successfully built according to Fig.2. In Fig.5, the air-gap flux densities B_1 of motor winding and B_2 of the levitation winding are calculated by the analytic method. The waveforms are shown with the radial displacements of the rotor shaft at the rated speed of 2700r/min.

CONCLUSION

The independent control between the levitation and drive subsystem is an effective way for bearingless induction motors in ultra-speed operation. In this paper, three methods of detecting the flux density vectors B_1 of the drive winding and B_2 of the levitation winding with search coils are proposed, as well as the control system configuration. In that case, not only the ultra-speed operation of the bearingless induction motor becomes possible, but also the effect on levitation controlling, which caused by the drive winding's parameters change or error, is avoided. The experimental results verify the validity of the proposed methods.

ACKNOWLEDGEMENT

The authors acknowledge the grant of National Nature Science Foundation of China (50377012), Aeronautical Science Foundation of China (K1600060603).

REFERENCES

[1] J.Bichsel. Beiträge zum lagerlosen Elektromotor. Diss. ETH Zürich Nr.9303, Zürich 1990

[2] A.Chiba, T.Deido, T.Fukao and M.A.Rahman. An analysis of bearingless AC motors. IEEE Trans. Energy Conversion, 1994, 9(1):61-68

[3] R.Schob and J. Bichsel. Vector control of the bearingless motor. In Proc.4th Int. Symp. Magnetic Bearings, Zürich, Switzerland. 1994:327-332

[4] A.Chiba, D.T.Power and M.A.Rahman. Analysis of no-load characteristics of a bearingless induction motor. IEEE Trans. Industry Application, 1995, 31(1):77-83

[5] Zhiquan Deng, Hongquan Zhang, Xiaolin Wang, et al. Nonlinear decoupling control of the bearingless induction motors based on the airgap motor flux orientation. Chinese Journal of aeronautics, 2002,15(1):38-43

[6] Xiaolin Wang, Zhiquan Deng, et al. Research and Developments of Bearingless Induction Motors. Acta Aeronautica et Astronautica Sinica. 2003. 24(3):259-262

[7] De Doncker, R.W. Novotny.D.W. The Universal Field Oriented (UFO) controller. IEEE Trans. Industry Applications. 1994, 30(1):92-100

[8] De Doncker, R.W.; Profumo, F.; Pastorelli, M.; Ferraris, P. Comparison of universal field oriented (UFO) controllers in different reference frames. IEEE Trans. Power Electron. 1995, 10(2):205-213

[9] K.Yasuda, T.Kuwajima, A.Chiba, et al. A proposed controller for bearingless induction drives with search coils wound around stator teeth. Maglev 2000, Rio de Janeiro, Brazil:.435-440

[10] Tadashi Satoh, Masaru Ohsawa, Satoshi Muri, et al. Bearingless rotary machine. United States Patent, 6078119. Jun.20, 2000.